JOC The Journal of Organic Chemistry

Article

pubs.acs.org/joc

High-Affinity RNA Targeting by Oligonucleotides Displaying Aromatic Stacking and Amino Groups in the Major Groove. Comparison of Triazoles and Phenyl Substituents

Pawan Kumar,[†] Mick Hornum,[†] Lise J. Nielsen,[†] Gérald Enderlin,[‡] Nicolai Krog Andersen,[†] Christophe Len,[‡] Gwénaëlle Hervé,[‡] Guillaume Sartori,[‡] and Poul Nielsen*[,†]

[†]Nucleic Acid Center, Department of Physics, Chemistry and Pharmacy, University of Southern Denmark, 5230 Odense M, Denmark

[‡]Transformations Intégrées de la Matière Renouvelable, UTC-ESCOM, Centre de recherche Royallieu, BP 20529, 60205 Compiègne, France

Supporting Information

ABSTRACT: Three 5-modified 2′-deoxyuridine nucleosides were synthesized and incorporated into oligonucleotides and compared with the previously published 5-(1-phenyl-1,2,3-triazol-4-yl)-2′-deoxyuridine monomer **W**. The introduction of an aminomethyl group on the phenyl group led to monomer **X**, which was found to thermally stabilize a 9-mer DNA:RNA duplex, presumably through the partial neutralization of the negative charge of the backbone. By also taking advantage of the stacking interactions in the major groove of two or more of the monomer **X**, an extremely high thermal stability was obtained. A regioisomer of the phenyltriazole substituent, that is the 5-(4-phenyl-1,2,3-triazol-1-yl)-2′-deoxyuridine monomer **Y**, was found to destabilize the DNA:RNA duplex significantly, but stacking in the major groove compensated for this when two to four monomers were incorporated consecutively. Finally, the 5-phenyl-2′-deoxyuridine monomer **Z** was incorporated for comparison, and it was found to give a more neutral influence on duplex stability indicating less efficient stacking interactions. The duplexes were investigated by CD spectroscopy and MD simulations.

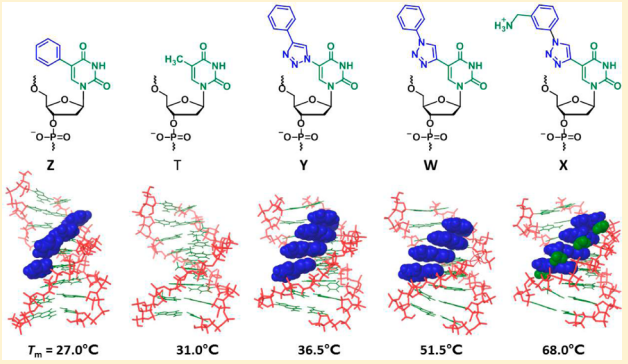

INTRODUCTION

Since its introduction in the late 1970s,[1] antisense technology has been seen as an attractive strategy to regulate gene expression by the use of short oligonucleotides (ONs) called antisense ONs which bind to their target RNA in a sequence specific manner.[2] Introduction of chemically modified nucleotides in antisense ONs has emerged as an important approach to increase their affinity and specificity toward RNA targets as well as their stability against nucleases.[3,4] One approach in this regard is the introduction of modified nucleobases capable of enhancing stacking interactions while maintaining the Watson–Crick base-pairing properties. For instance, replacement of cytosine with phenoxazine has been shown to increase the thermal stability of a DNA:RNA duplex significantly.[5] Another example is the 5-propynylpyrimidine nucleoside modification, which has also been shown to increase the thermal duplex stability by taking advantage of better stacking interactions.[6,7]

Recently, we introduced the modified nucleoside monomer **W** (Figure 1) in which a phenyltriazole group is attached to the 5-position of 2′-deoxyuridine.[8] This monomer is very conveniently synthesized by using the Cu(I)-catalyzed alkyne–azide cycloaddition (CuAAC) reaction,[9,10] which has been recently used intensively in nucleic acid chemistry.[11−17]

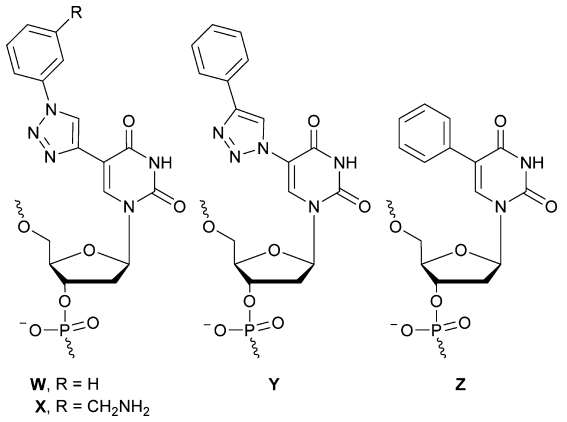

Figure 1. Structure of 5-functionalized 2′-deoxyuridine monomers.

Consecutive incorporations of monomer **W** led to the formation of very stable DNA:RNA duplexes through efficient stacking between the phenyltriazole moieties in the major

Received: November 22, 2013
Published: March 10, 2014

   dx.doi.org/10.1021/jo4025896 | J. Org. Chem. 2014, 79, 2854−2863

groove.[8] Thus, two consecutive incorporations of **W** gave an increase in melting temperature of a 9-mer DNA:RNA duplex of 3.3 °C per modification, and this increased to 5.1 °C per modification with four consecutive incorporations.[8,18] The scope of this DNA analogue was further extended with the introduction of the corresponding 2′-deoxycytidine monomer, which was also found to participate in stacking interactions in the major groove.[19] Furthermore, the ONs modified with these monomers were found to be resistant toward degradation by nucleases.[19] In an effort to optimize the stacking interactions in the major groove, we have introduced various substituted phenyltriazoles.[18] A sulfonamide substituent on the phenyl ring of **W** was shown to give a slight further increase in the thermal stabilization of the DNA:RNA duplexes, i.e., a maximum increase in melting temperature of 6.1 °C per modification with four consecutive incorporations as compared to the 5.1 °C obtained with **W**.[18,20] For the present study, we decided to further explore the scope of the phenyltriazole building block **W** by (1) introducing a positively charged substituent to the phenyltriazole (monomer **X**, Figure 1), (2) varying the substitution pattern of the triazole ring (monomer **Y**, Figure 1), and (3) replacing the phenyltriazole substituent with a simpler phenyl group (monomer **Z**, Figure 1).

By the introduction of monomer **X** (Figure 1), we expected to stabilize DNA:RNA duplexes even further by combining the efficient stacking of the phenyltriazole moieties in the major groove with electrostatic interactions between the positively charged amino group and the negatively charged phosphodiester backbone. Hence, previous results with nucleotide monomers modified with an aminopropynyl group at the 5-position of 2′-deoxyuridine have been shown to form thermally and enzymatically stable duplexes through a similar combination.[21,22] However, we have recently shown that stacking efficiency of triazoles attached to the 5-position of 2′-deoxyuridine is significantly higher than alkynyl substituents in the same position,[20] and we therefore expected **X** to reveal duplexes of very high thermal stability.

The monomer **Y** (Figure 1) is an analogue of **W** in which the phenyl group is attached to the 5-position of the 2′-deoxyuridine through an inversed triazole, i.e., the 5-position of the uracil is connected to the *N*-1 position of the triazole ring rather than the *C*-4 position. Therefore, a comparison can be drawn between the normal phenyltriazole (monomer **W**) and the inversed phenyltriazole (monomer **Y**) in terms of their ability to participate in stacking interactions in the major groove. Furthermore, it is interesting to explore not only the 5-ethynyl modified pyrimidine nucleosides as a component for nucleic acid click chemistry reactions, but also the 5-azido-modified pyrimidine nucleosides. In order to further understand the role of the triazole in the stacking interactions in the major groove, we also decided to completely remove the triazole linker and introduce monomer **Z** (Figure 1) with a phenyl group directly attached to the 5-position of 2′-deoxyuridine.

RESULTS AND DISCUSSION

Chemical Synthesis. For the introduction of the monomers **X**, **Y**, and **Z**, we synthesized the three 5′-*O*-DMTr-protected 3′-*O*-phosphoramidites **3**, **7**, and **11**, respectively (Scheme 1), as suitable starting materials for solid phase oligonucleotide synthesis. The first two are based on the general concept of the Cu(I)-catalyzed azide−alkyne cycloaddition (CuAAC).[9,10] The well-known 5′-*O*-DMTr-protected 5-ethynyl-2′-deoxyuridine **1**[23] was reacted with *N*-(3-bromobenzyl)-2,2,2-trifluoroacetamide using our formerly published in situ azidation/CuAAC protocol[8] to obtain nucleoside **2**. Phosphitylation using standard conditions afforded the phosphoramidite **3**. 5-Azido-2′-deoxyuridine **4** was prepared in three high-yielding steps from 5-bromo-2′-deoxyuridine using a literature procedure.[24] DMTr-protection of **4** gave **5** and subsequent CuAAC reaction with commercially available phenylacetylene furnished nucleoside **6** in good yield. Standard phosphitylation of this nucleoside afforded the phosphoramidite **7**. Finally, 5-phenyl-2′-deoxyuridine **9**[25,26] was prepared by a Suzuki−Miyaura coupling between commercially available 5-iodo-2′-deoxyuridine **8** and phenylboronic acid.[26] Subsequent DMT protection afforded **10**, and phosphitylation gave the required phosphoramidite **11**. The identities of the compounds were fully ascertained by NMR spectroscopy (^{1}H, ^{13}C, ^{31}P, COSY, HSQC, and/or HMBC) and high-resolution mass spectrometry.

Scheme 1[a]

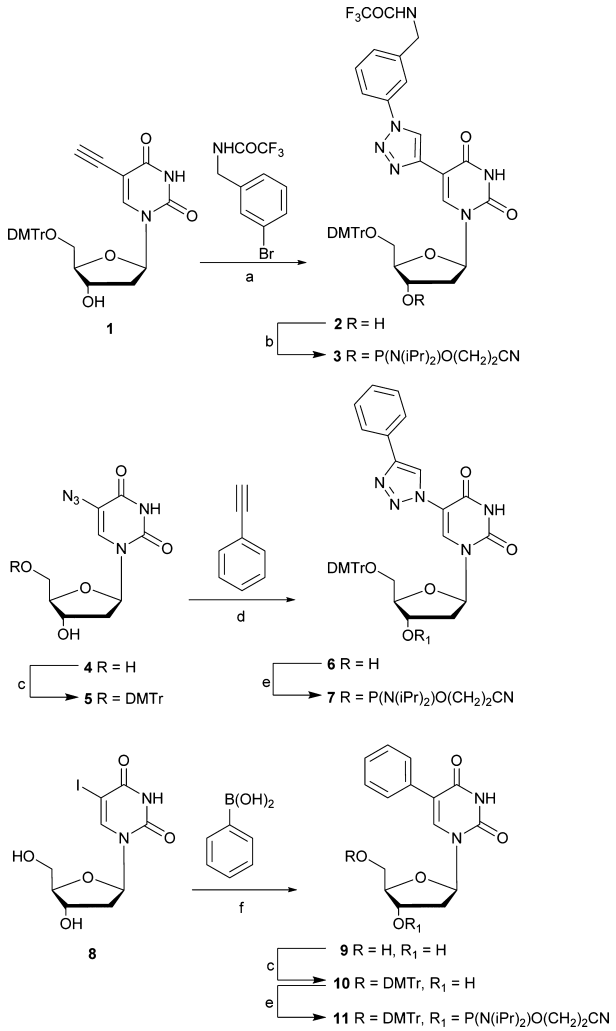

[a]Reagents and conditions: (a) NaN_3, *N,N*-dimethylethylenediamine, CuI, $EtOH/H_2O$, MW 100 °C, Na ascorbate, 72%; (b) $NC(CH_2)_2OPClN(i\text{-}Pr)_2$, $(i\text{-}Pr)_2NEt$, CH_2Cl_2, 54%; (c) DMTrCl, pyridine, 42% **5**, 47% **10**; (d) $CuSO_4{\cdot}5H_2O$, Na ascorbate, pyridine/H_2O/*t*BuOH (1:2:2, v/v/v), 65%; (e) $NC(CH_2)_2OPClN(i\text{-}Pr)_2$, $EtN(i\text{-}Pr)_2$, $(ClCH_2)_2$, 67% **7**, 66% **11**; (f) Na_2PdCl_4 (0.1 mol %), KOH, H_2O, MW, 100 °C, 85% (ref 26).

dx.doi.org/10.1021/jo4025896 | J. Org. Chem. 2014, 79, 2854−2863

Hybridization Studies. The phosphoramidites **3**, **7**, and **11** were successfully incorporated into ONs to give the modified nucleotide monomers **X**, **Y**, and **Z**, respectively, using an automated DNA synthesizer with tetrazole as the activator. Standard conditions were employed except for extended coupling times (15 min) for the modified phosphoramidites. The ON sequence chosen for the present study is a T-rich 9-mer sequence similar to our previous studies with monomer **W**.[8,18] ONs with one to four consecutive incorporations of monomers **X**, **Y**, or **Z** (Table 1, entries 6−17) and mixed incorporations of **X**, **Y**, or **Z** with **W** (entries 18−22) were prepared. Constitution and purity of the synthesized ONs was verified by MALDI-TOF MS analysis and ion-exchange chromatography, respectively. The ONs were mixed in medium salt buffer with complementary single-stranded RNA or single-stranded DNA. Melting temperatures (T_m) of the resulting duplexes were derived from the UV melting curves at neutral pH 7 and compared with the T_m of the corresponding unmodified duplex (Table 1, entry 1), and differences in melting temperature per modification (ΔT_m/mod) were determined (Table 1, entries 2−22).

Table 1. Hybridization Data for the Duplexes Featuring the Monomers W, X, Y, or Z

		T_m[a] (°C) (ΔT_m per modification (°C))[b]	
entry	ON sequences	compl RNA	compl DNA
1	5′-d(GTGTTTTGC)	31.0	33.0
2	5′-d(GTGT**W**TTGC)	29.0 (−2.0)[c]	28.0 (−5.0)[c]
3	5′-d(GTGT**WW**TGC)	37.5 (+3.3)[c]	30.5 (−1.5)[c]
4	5′-d(GTG**WWW**TGC)	43.0 (+4.0)[c]	30.0 (−1.0)[c]
5	5′-d(GTG**WWWW**GC)	51.5 (+5.1)[c]	32.0 (−0.3)[c]
6	5′-d(GTGT**X**TTGC)	33.5 (+2.5)	31.0 (−2.0)
7	5′-d(GTGT**XX**TGC)	45.5 (+7.0)	33.5 (+0.2)
8	5′-d(GTG**XXX**TGC)	59.0 (+9.3)	41.0 (+2.7)
9	5′-d(GTG**XXXX**GC)	68.0 (+9.2)	45.0 (+3.0)
10	5′-d(GTGT**Y**TTGC)	24.5 (−6.5)	25.0 (−8.0)
11	5′-d(GTGT**YY**TGC)	29.0 (−1.0)	23.5 (−5.0)
12	5′-d(GTG**YYY**TGC)	31.0 (0.0)	21.5 (−3.8)
13	5′-d(GTG**YYYY**GC)	36.5 (+1.4)	21.5 (−2.9)
14	5′-d(GTGT**Z**TTGC)	26.5 (−4.5)	30.5 (−3.0)
15	5′-d(GTGT**ZZ**TGC)	25.0 (−3.0)	27.5 (−2.7)
16	5′-d(GTG**ZZZ**TGC)	25.0 (−2.2)	28.0 (−1.7)
17	5′-d(GTG**ZZZZ**GC)	27.0 (−1.0)	25.5 (−1.9)
18	5′-d(GTG**WXW**TGC)	47.0 (+5.3)	33.0 (0.0)
19	5′-d(GTG**XWX**TGC)	50.0 (+6.3)	35.5 (+1.2)
20	5′-d(GTG**XWWX**GC)	57.0 (+6.5)	41.0 (+2.0)
21	5′-d(GTG**WYW**TGC)	38.0 (+2.3)	25.5 (−2.5)
22	5′-d(GTG**WZW**TGC)	29.5 (−0.5)	25.5 (−2.5)

[a]Melting temperatures are obtained from the maxima of the first derivatives of the melting curves (A_{260} vs temperature) recorded in a medium salt buffer (Na_2HPO_4 (2.5 mM), NaH_2PO_4 (5 mM), NaCl (100 mM), EDTA (0.1 mM), pH 7.0) using 1.5 μM concentrations of each strand. Complementary target sequences are 5′-GCA AAA CAC (RNA or DNA). [b]The changes in melting temperature for each modification as compared to the unmodified reference duplex (entry 1) are shown in parentheses. [c]Data taken from refs 8 and 18.

A single incorporation of monomer **X** in the center of a 9-mer DNA:RNA duplex was found to increase the thermal stability of the duplex by 2.5 °C (entry 6) compared to the unmodified duplex (entry 1). For comparison, monomer **W** decreases the duplex stability by 2.0 °C in the same sequence context (entry 2). This indicates that the thermal penalty due to a single phenyltriazole group is compensated by the aminomethyl group in monomer **X**. Interestingly, very stable DNA:RNA duplexes were observed for the ONs featuring two to four consecutive incorporations of **X** (ΔT_m in the range of +7.0 to +9.3 °C per modification, entries 7−9) compared to the unmodified duplex. Therefore, the effect was stronger than what was seen for monomer **W** (ΔT_m from +3.3 to +5.1 °C per modification, entries 2−4) and other 5-triazole-substituted 2′-deoxyuridines.[8,18,20] This indicates for monomer **X** that the efficient stacking of the phenyltriazole moieties in the major groove are combined with partial neutralization of the negatively charged backbone by the aminomethyl group to give the very stable duplexes. When introduced in the center of a 9-mer dsDNA, monomer **X** decreases the thermal stability of the duplex (ΔT_m = −2.0 °C, entry 6) compared to the unmodified duplex. However, this decrease is smaller than that was seen for **W** in the similar context (ΔT_m = −5.0 °C, entry 2). With three or four consecutive incorporations of monomer **X**, stabilized duplexes were observed (entries 8 and 9, ΔT_m/mod =2.7−3.0 °C) in contrast to what was seen for monomer **W** in the similar sequences (entries 2−4). These data further support that the aminomethyl group is increasing the thermal stability of the duplexes by partially neutralizing the negative charge of the backbone.

A single incorporation of monomer **Y** featuring an inversed triazole moiety causes a penalty of 6.5 °C (entry 10) in the thermal stability of the modified DNA:RNA duplex compared to the unmodified duplex (entry 1). This is in contrast to monomer **W** which causes a drop of only 2.0 °C (entry 2). This suggests that phenyltriazoles are better accommodated in DNA:RNA duplexes when connected to the nucleoside through the *C*-4 position of the triazole ring rather than the *N*-1 position. A second adjacent incorporation of **Y** partially compensates the thermal penalty from the single incorporation (compare ΔT_m/mod of −6.5 °C, entry 10, with ΔT_m/mod of −1.0 °C, entry 11) indicating favorable stacking interactions between the two inversed phenyltriazole moieties (monomer **Y**) in accordance with the property of the regular phenyltriazole moiety (monomer **W**). A duplex with intact thermal stability was observed for three consecutive incorporations of **Y** (entry 12), and four consecutive incorporations of **Y** gave a DNA:RNA duplex with increased thermal stability (entry 13, ΔT_m/mod = +1.4 °C). These observations strongly suggest that the inversed phenyltriazole group from monomer **Y** has the ability to participate in stacking interactions when incorporated more than once in the center of a DNA:RNA duplex. However, the thermal penalty caused by the introduction of each monomer **Y** (entry 10) counteracts the positive effect of stacking interactions. When introduced in the center of the 9-mer dsDNA (entry 10), monomer **Y** induced a drop of 8.0 °C in the thermal stability as compared to 5.0 °C for monomer **W** (entry 2). Thus, also in dsDNA, monomer **W** is better accommodated than **Y**, and in duplexes with two to four consecutive incorporations of **Y** the thermal penalty per modification decreases only from 8.0 to 2.9 °C (entries 10−13).

The single incorporation of monomer **Z** led to the destabilization of the modified DNA:RNA duplex by 4.5 °C and of the dsDNA duplex by 3.0 °C compared to the unmodified duplexes (entry 14). Therefore, **Z** is better accommodated in both duplexes than **Y**. On the other hand, two to four consecutive incorporations of **Z** in the center of the

dx.doi.org/10.1021/jo4025896 | J. Org. Chem. 2014, 79, 2854−2863

duplex did not compensate for this to the same extent since the thermal penalty per modification decreases only from 4.5 to 1.0 °C in the DNA:RNA duplex (entries 14−17). This suggest that stacking interactions between phenyl groups in the major groove from monomer **Z** are present but weaker than for the triazoles. In general, a similar behavior of **Z** was observed for the corresponding dsDNA duplexes.

A graphical presentation of how the ΔT_m per modification varies with one to four incorporations of **W**, **X**, **Y**, or **Z** in the center of a 9-mer DNA:RNA duplex is shown in Figure 2. In

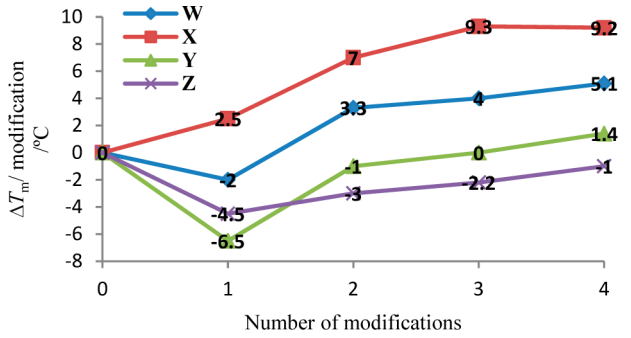

Figure 2. Graphical illustration of ΔT_m vs the number of incorporations.

going from one incorporation of the monomers **W**, **X**, or **Y** to two adjacent incorporations, ΔT_m/mod increases by around 5 °C. This clearly suggests for the similar strong stacking efficiency of regular phenyltriazole (monomers **W** and **X**) and inversed phenyltriazole (monomer **Y**) in the major groove. In a similar context, monomer **Z** induced a smaller increase of only 1.5 °C in the ΔT_m/mod value indicating a favorable but smaller stacking interaction between the phenyl groups. In general, the effect of the third and fourth incorporation was found to be similar for **W**, **X**, or **Y**, reflecting their similar efficiency to stack. The ΔT_m/mod for **X** is found to be around 4−5 °C higher than for **W** in all the studied duplexes, demonstrating the positive effect of the aminomethyl group on the thermal stability of the duplexes.

Next, ONss with mixed consecutive incorporations of monomer **X**, **Y**, or **Z** with **W** were studied in order to illuminate the interplay between the different monomers (Table 1, entries 18−22). ONs featuring mixed consecutive incorporations of monomer **W** and **X** form duplexes with complementary RNA or DNA strands, which are generally more thermally stable than the duplexes featuring the same number of modifications of **W** (compare entries 18 and 19 with entry 4, and entry 20 with 5). These data support that monomer **X** is cooperatively participating in the stacking interactions with **W** and that the aminomethyl group is inducing further stabilization of the duplex, presumably by partially neutralizing the negative charge of the backbone. In comparison with the entries 7−9, however, it is also clear that this additional increase in stability by the amino group is independent of the placement in the sequence and can be obtained uncompromised on two consecutive phenyltriazoles. The ON featuring one **Y** in between two **W**'s on hybridization with the complementary RNA strand forms a duplex with a thermal stability higher that the unmodified duplex as well as the duplex with three **Y**s in the center (compare entry 21 with 1 and 12, respectively). This indicates that the inversed phenyltriazole from monomer **Y** can stack with the phenyltriazole from monomer **W**. However, a drop of 5.0 °C in the T_m was observed when compared to the duplex with three consecutive incorporations of monomer **W** (compare entry 21 with entry 4) in accordance to the negative influence of each individual inverse phenyltriazole on thermal stability. The combination of a monomer **Z** in between two **W**'s leads to a DNA:RNA duplex with neutral thermal stability indicating that the phenyl group is hampering the stacking in the major group significantly.

Finally, we investigated the fidelity in the RNA recognition for the ONs, which form the most stable duplexes with complementary RNA targets, i.e., with four consecutive incorporations of **X** or with mixed incorporations of **W** and **X** (Table 2). These ONs were hybridized with RNA targets featuring a centrally placed mismatch nucleotide, and as expected, mismatched duplexes were found to be less stable than the matched duplex. The C mismatch nucleotide was best discriminated (ΔT_m in the range of −20.0 to −27.5 °C) followed by the U mismatch nucleotide (ΔT_m in the range of −15.0 to −20.5 °C) and the G (ΔT_m in the range of −8.5 to −11.0 °C). This is parallel to what was observed for monomer **W** and other 5-triazole substituted 2′-deoxyuridine monomers studied.[8,18,20]

CD Spectroscopy. The global conformation of DNA:RNA duplexes featuring four consecutive incorporations of monomers **X**, **Y**, or **Z** (Table 1, entries 9, 13, and 17) and four consecutive mixed incorporations of **X** with **W** (entry 20) were investigated by CD spectroscopy. CD spectra were recorded at 10 °C in a medium salt buffer by using 3.0 μM of each strand (Figure 3). As expected, the CD spectrum of the unmodified DNA:RNA duplex (entry 1) was found to adopt intermediate A/B-type geometry with characteristic bands from both geometries. Thus, a positive band at 265 nm (A-type) with a shoulder at 282 nm (B-type) was observed along with a positive band at 220 nm (B-type) and negative bands at 247 nm (B-

Table 2. Hybridization Data for the Mismatched Duplexes

		T_m /°C[a] (ΔT_m /°C[b]) 3′-r(CAC A**B**A ACG)			
entry	ON sequences	B = A	B = C	B = G	B = U
1	5′-d(GTG**WWWW**GC)	51.5	24.0[c] (−27.5)	42.0[c] (−9.5)	31.0[c] (−20.5)
2	5′-d(GTG**XXXX**GC)	68.0	42.0 (−26.0)	57.0 (−11.0)	49.0 (−19.0)
3	5′-d(GTG**XWWX**GC)	57.0	37.0 (−20.0)	48.5 (−8.5)	42.0 (−15.0)

[a]See Table 1. [b]Mismatch studies. The changes in melting temperature as compared to the matched duplex are shown in parentheses. [c]Data taken from ref 8.

dx.doi.org/10.1021/jo4025896 | J. Org. Chem. 2014, 79, 2854−2863

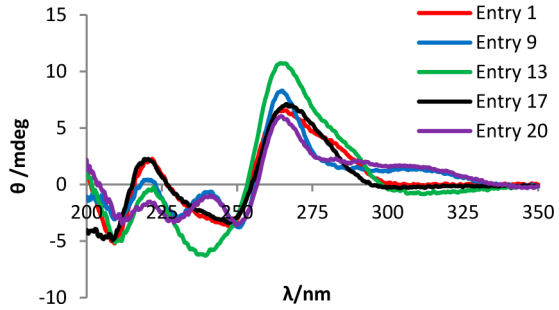

Figure 3. CD spectra of selected DNA:RNA duplexes. Entry numbers refer to Table 1.

type) and 210 nm (A-type). After establishing the geometry of the unmodified duplex as the mixed A/B type, the effect of the modified monomers on the duplex geometry was studied. The duplex featuring four consecutive incorporations of **X** (entry 9) displayed a positive band at 265 nm and two negative bands at 251 and 210 nm suggesting the overall A/B type duplex geometry. However, the positive band at 220 nm observed in the CD spectrum of the unmodified duplex was very small. This is in accordance with what was seen for monomer **W** (entry 5).[8] Furthermore, a very broad band with a center at around 311 nm and a new negative band at 230 nm were also observed (entry 9). These new bands observed for **X** were not seen in the CD spectrum of **W** in the similar sequence context,[8] and their appearance might be due to local changes in the conformation of the duplex by interactions of the aminomethyl group with the backbone. The CD spectrum recorded for the duplex featuring mixed incorporations of **W** and **X** (entry 20) was very similar. The CD spectrum and thereby the overall duplex geometry of the duplex featuring four consecutive incorporations of **Y** (entry 13) was found to be generally similar to the unmodified duplex with an intense positive band at 265 nm, a shoulder at 280 nm and a negative band at 210 nm. Small variations were observed as the band at 265 nm is more intense, the band at 220 nm is smaller and the negative band at 247 nm is shifted toward shorter wavelength and appeared at 238 nm. It is interesting to note that for monomers **W** and **X**, this band is shifted toward longer wavelength and appeared at 251 nm. The CD spectrum of the duplex with four consecutive incorporations of **Z** (entry 17) was very similar to the one from the unmodified duplex indicating no major influence on duplex geometry from this modification.

Molecular Modeling. In order to get a better understanding of the preferred conformations of the monomers **W**, **X**, **Y**, and **Z**, we used ab initio calculations on three model structures to find the torsions θ, φ, and ω (see Figure 4) of the 5-substituents relative to the uracil. The 5-substituent should align in the same plane as the uracil for π-overlap such that the most efficient stacking is achieved. In order to reduce the computational burden to a feasible level while retaining the

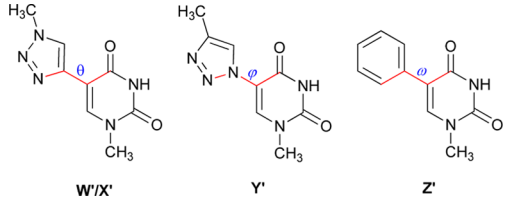

Figure 4. Structures of model compounds **W′**/**X′**, **Y′**, and **Z′**.

accuracy of calculation (MP2 using 6-31G(d,p) basis sets), the 2′-deoxyribose moieties were replaced by methyl groups, and the phenyltriazoles were replaced by methyltriazoles, to get the simplified model compounds **W′**/**X′**, **Y′**, and **Z′**.

The obtained energy profiles are shown in Figure 5. In agreement with our former results,[8] the energy profile for **W′**/

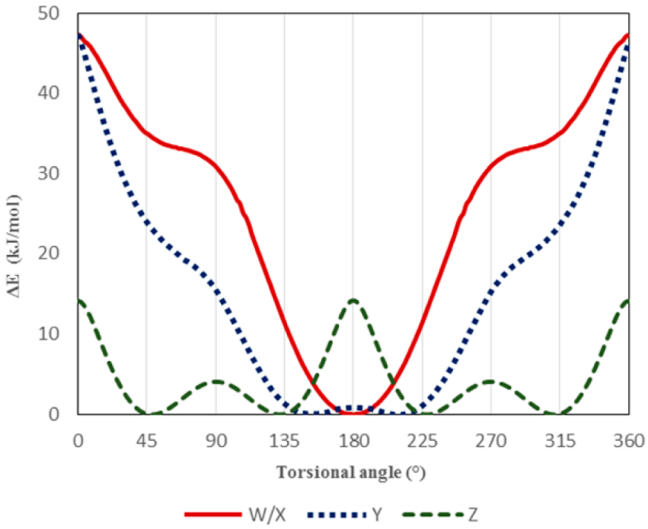

Figure 5. Dihedral MP2 scans of the bonds connecting the triazoles or the phenyl to the pyrimidine (see Figure 4) using 2° increments.

X′ has a global minimum in θ = 180°, corresponding to a strong preference for the molecule to adopt a coplanar conformation with a CH−O interaction from the triazole-C5 to the uracil-O4. When the triazole ring is inversed as in **Y′**, the preferred conformation surprisingly becomes antiperiplanar, with the global minimum shifted about ±32° away from coplanarity (φ = 148° and 212°). The coplanar conformation (φ = 180°) is, however, only slightly higher in energy (+0.86 kJ/mol) and the curve of **Y′** is essentially flat from φ = 145° to φ = 215°, indicating that **Y′** has a higher degree of freedom compared to **W′**. The calculated barrier to rotation happens to be almost identical for **W′**/**X′** and **Y′** (~47 kJ/mol). When the triazole ring is entirely removed and replaced by a phenyl group as in **Z′**, the coplanar conformations (ω = 0° and ω = 180°) become global maxima and the perpendicular conformations (ω = 90° and ω = 270°) are local maxima. In fact, the lowest energy structures correspond to an inclination of 45° or 135° of the phenyl substituent. It is also significant that the rotational barrier for **Z′** is much smaller (~14 kJ/mol) than that of the triazolated molecules. Altogether, these results suggest that while **W** and **X** should strongly prefer coplanar conformations, **Y** is more flexible around coplanarity, whereas the phenyl ring of **Z** is not prone to align in the same plane as the pyrimidine indicating that it could lead to poor stacking interaction in duplexes.

To get more information about how well multiple incorporations of **W**, **X**, **Y**, and **Z** are accommodated in the DNA:RNA duplexes, molecular dynamics (MD) simulations were performed. Specifically, these simulations may provide an indication of the efficiency of stacking in the major groove as well as the effects of the modifications on the duplex geometry. In the case of **X**, an idea about the positioning of the positive charges that arise from the methylamines might also be obtained. Using a simulation time of 5 ns, a reasonable

dx.doi.org/10.1021/jo4025896 | J. Org. Chem. 2014, 79, 2854−2863

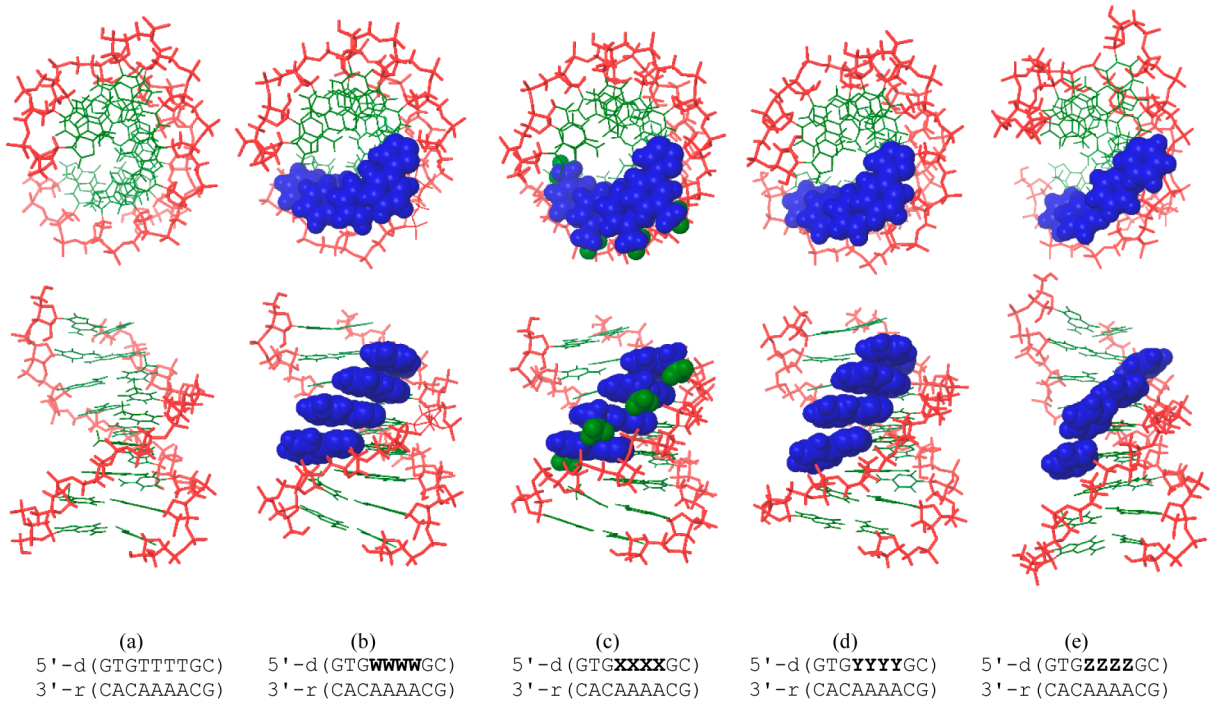

Figure 6. Global minimum structures obtained by 5 ns MD simulations of the DNA:RNA duplexes corresponding to entries 1, 5, 9, 13, and 17 in Table 1. The last was performed at 10 °C and the other four at 27 °C. The backbone is shown in red, nucleobases in green, and 5-substituents in space-filling blue, except for the amino groups, which are shown in space-filling green.

estimation of the global minimum for the duplex can be found. The structure of the 9-mer duplex featuring four consecutive **W** residues (entry 5, Table 1) have been modeled before,[8] and we decided to use this minimized structure as a benchmark for the duplexes containing four residues of either **X**, **Y**, or **Z** (entries 9, 13, and 17, Table 1). The obtained global minima structures are shown in Figure 6. In addition, the duplex containing three **X**'s (entry 8) or two **Z**s (entry 15) as well as the duplex containing mixed residues of **X** and **Z** (entry 20) were studied (see the structures in Figure S1, Supporting Information).

In our previous studies,[8] four consecutive **W**'s in the 9-mer duplex have been shown to give efficient stacking in the major groove, and this is now augmented by the present MD simulation (Figure 6b). When four consecutive **X**'s are introduced (Figure 6c), the amino groups of the 5-substituents appear to neutralize the negatively charged phosphates of the complementary DNA strand (for a close-up, see Figure S2, Supporting Information). In addition, there appears to be efficient stacking between the three upmost **X**'s in a similar degree to the **W**'s, but notably, the 5′-end **X** appears to rotate around the phenyl−triazole bond and slide to the side in order to neutralize the backbone charge rather than engage in stacking interactions. This might explain why the fourth incorporation does not improve the relative increase in thermal stability even further (see Figure 2). With three consecutive **X**'s (entry 8) (Figure S1, Supporting Information), all three participate in stacking as well as neutralization of phosphates in the same way as the first three **X**'s from the 3′-end of the four in entry 9. When the **XWWX** motif was applied to the MD simulation (Figure S1, Supporting Information), a certain bending of the substituents was observed that allowed some degree of stacking. While the 3′-end **X** residue still neutralizes the phosphate charge of the DNA strand like in the case of four **X**'s (Figure 6c), the 5′-**X** residue of the **XWWX** motif unexpectedly appears to "cross-link" the two strands to neutralize the phosphate charge of the RNA strand. In general, all simulations of duplexes containing **X** shows coplanarity of the triazole and the uracil corresponding to torsional angles θ (Figures 4 and 5) of 160−181°, which is, however, deviating more from the optimal 180° than in the case of the **W**'s (θ = 173−185°). In the case of **Y** (Figure 6d), there is indeed stacking between the **Y**'s as suggested by the T_m values, although the efficiency of the stacking may not be as clear as in the case of the **W** residues (Figure 6b). Specifically, there appears to be a slight bending of the two lowermost residues. The torsional angles φ, however, are 173−183°. Most strikingly, the introduction of four **Z**'s appears to induce a slight unwinding of the helix (Figure 6e), probably caused by the tilting of the phenyl substituents. Hence, the angles of the phenyluracil are from 211 to 217° not far from the optimal as seen in Figure 5. Therefore, efficient stacking is probably prohibited.

DISCUSSION

In this study, we have introduced three new 5-substituted-2′-deoxyuridine nucleotide monomers, **X**, **Y**, and **Z**, into ONs. The syntheses of all three are easy and based on well-established organometallic reactions, either the CuAAC or the Suzuki−Miyaura reaction, and the phosphoramidite building blocks are obtained in only four to six steps from commercially available nucleoside precursors. From the hybridization study it is clear that monomer **X** displays by far the highest melting temperatures when introduced in both DNA:RNA and dsDNA duplexes. In particular, DNA:RNA duplexes are extremely stable with consecutive incorporations of **X** and consistently found to be more stable than corresponding duplexes modified with **W**. This demonstrates that the very strong RNA-targeting behavior found for **W** and analogues thereof[8,18−20] can be even further improved by the additive effect of the stacking

dx.doi.org/10.1021/jo4025896 | J. Org. Chem. 2014, 79, 2854−2863

interactions from the 5-phenyltriazole moiety and of the aminomethyl group, which presumably leads to charge neutralization of the backbone. This further consolidates the potential of the phenyltriazole pyrimidine modification for the development of antisense oligonucleotides, as the RNA affinity can be tuned by the number of consecutive incorporations of monomer **W** as well as by the number of aminomethyl groups by using monomer **X**. It is an important observation that by the use of **X** in contrary to **W**, an increased DNA:RNA duplex stability can even be obtained by a single incorporation of the phenyltriazole (see Table 1 and Figure 2). Future structural and physicochemical studies are needed to finally confirm the charge neutralization from the aminomethyl group of **X**. We have earlier proved that also the cytidine analogue with a phenyltriazole substituent can increase the duplex stability so that mixed purine RNA sequences can be targeted.[19] Furthermore, the phenyltriazoles significantly stabilize the ONs against degradation under physiological conditions.[19]

Obviously, the potential of the regioisomeric monomer **Y** is hampered by the large decrease in duplex stability associated with each incorporation. Even though this is compensated (Table 1, Figure 2) by efficient stacking interactions, the potential for antisense purposes is small as compared to **W**. Nevertheless, it is a very important observation that the substitution pattern of the triazole substituents displays a large impact on the resulting duplexes. Hence, several studies have used the CuAAC reaction and a triazole at the 5-position of uracil as the attaching point for, e.g., labeling ONs mostly through the 5-ethynyluracil[27] but recently also through the in situ generated 5-azidouracil moiety.[28] Hence, it is important to know that the thermal penalty of introducing a single triazole into a dsDNA or a DNA:RNA duplex is very high if the triazole is "inversed" (as in **Y**) and somewhat smaller if not (as in **W** and **X**). Likewise, direct attachment of aromatics, like substituted phenyl groups, has been applied before for different purposes, incl. labeling.[29] Hereby, it is an interesting observation that an isolated **Z** is better accommodated in the duplexes than **Y**, and in the case of dsDNA, also better than **W**. Therefore, Suzuki−Miyaura couplings of phenyls can be a better choice than the CuAAC reaction for labeling ONs if the thermal stability of the subsequent duplexes is an issue.

In the present study, we have applied CD spectra and molecular modeling in order to enlighten the different behavior of the monomers **X**, **Y**, **Z**, and **W** in DNA:RNA duplexes. Hence, it is very clear that the stacking of the substituents in the major groove is the key to the high stability of the duplexes. For the phenyltriazoles in **W** and **X**, there is a very strong preference for a coplanar conformation (see Figure 5) due to a CH−O interaction, and the MD simulation confirms the coplanarity also in the duplexes. Furthermore, this is not hampered by the introduction of aminomethyl groups and the subsequent neutralization of the phosphates. In fact, the synergy of stacking and charge neutralization leads to the extraordinary duplex stability, and this works despite consecutive incorporations of several amino groups. Monomer **Y** is apparently not restricted in the coplanar conformation (see Figure 5) and prefers in fact a 45° angle between the two aromatics. This might be the reason why the first introduction of **Y** is very unfavorable for the duplex, whereas stacking interactions between several substituents can force these into a coplanar conformation and eventually stabilize the duplexes. The fact that the coplanar conformation of the phenyl uracil is a local maximum (see Figure 5) is closely connected to the very imperfect stacking interactions of **Z**. The MD simulations (see Figure 6) support this and show a duplex conformation that is closer to the unmodified DNA:RNA duplex than to the triazole-modified duplexes, an indication that is fully confirmed by the CD spectrum. The small compensation in duplex stability obtained for several incorporations of **Z** might be due to hydrophobic effects rather than stacking interactions.

CONCLUSION

The combination of stacking interactions from the phenyltriazole group and charge neutralization through aminomethyl substituents in the major groove led to extraordinary stable DNA:RNA duplexes using consecutive incorporations of monomer **X**. This makes the combination of **X** and **W** and analogues thereof a strong and simple tool for the search for therapeutic oligonucleotides. Furthermore, it shows that with the right linkage, long arrays of aromatic groups can be arranged in the duplex major groove without compromising duplex stability and structure. Although the "inversed" triazole monomer **Y** is efficiently synthesized and can partake in similar stacking interactions in the major groove, the thermal penalty for a single incorporation is higher. The phenyl group of **Z** is better accommodated in the duplexes, although stacking interactions in the major groove are weaker. Hereby, this study presented the first direct comparison of the stacking interactions of the 5-phenyltriazole and 5-phenyl groups establishing a clear correlation between coplanarity of the aromats, the ability for stacking and the increase in duplex stability. The importance of the *C*-connected triazole group at the 5-position as in **W** and **X** for optimum stacking interactions is clear. Therefore, the present study demonstrates how delicately the decoration of nucleic acids is connected to duplex structure and stability.

EXPERIMENTAL SECTION

General Methods. All commercial reagents were used as supplied except CH_2Cl_2, which was distilled prior to use. Anhydrous solvents were dried over 4 Å activated molecular sieves (CH_2Cl_2, pyridine, and 1,2-dichloroethane) or 3 Å activated molecular sieves (DMF, CH_3CN). Reactions were carried out under argon when anhydrous solvents were used. All mixtures of solvents were prepared as a volume to volume ratio (v/v). All reactions were monitored by TLC using Merck silica gel plates (60 F_{254}). To visualize the plates, they were exposed to UV light (254 nm) and/or immersed in a solution of 5% H_2SO_4 in MeOH (v/v) followed by charring. Column chromatography was performed with silica gel 60 (particle size 0.040−0.063 μm, Merck). Silica gel was pretreated with 1% pyridine in CH_2Cl_2 (v/v) for the purification of 4,4′-dimethoxytrityl-protected nucleosides. ^{1}H NMR, ^{13}C NMR and ^{31}P NMR spectra were recorded at 400 MHz, 101, and 162 MHz, respectively. Chemical shift values (δ) are reported in ppm relative to either tetramethylsilane (^{1}H NMR) or the deuterated solvents as internal standard for ^{13}C NMR (δ: $CDCl_3$ 77.16 ppm, DMSO-d_6 39.52 ppm), and relative to 85% H_3PO_4 as external standard for ^{31}P NMR. 2D spectra (^{1}H−^{1}H COSY, and ^{1}H−^{13}C HSQC) have been used in assigning ^{1}H and ^{13}C NMR signals. High-resolution ESI (quadrupole) mass spectra were recorded in positive ion mode.

N-(3-Bromobenzyl)-2,2,2-trifluoroacetamide. A solution of 3-bromobenzylamine (0.63 mL, 5 mmol) and triethylamine (2.5 mL, 15 mmol) in CH_2Cl_2 (30 mL) was stirred at 0 °C, and a solution of trifluoroacetic anhydride (1.42 mL; 10 mmol) in CH_2Cl_2 (5 mL) was added. The reaction mixture was stirred at room temperature for 18 h and then washed sequentially with a 1 M aqueous solution of HCl and a saturated aqueous solution of $NaHCO_3$. The combined organic fraction was dried (Na_2SO_4) and then concentrated under reduced pressure. The residue was recrystallized from petroleum ether to afford

dx.doi.org/10.1021/jo4025896 | J. Org. Chem. 2014, 79, 2854−2863

the product as white needles (1.06 g; 75%): R_f 0.4 (ethyl acetate/petroleum ether, 4:1 v/v); mp 59 °C; ^{1}H NMR (400 MHz, DMSO-d_6) δ = 10.04 (br s, 1H, NH), 7.51−7.48 (m, 2H, Ar), 7.36−7.29 (m, 2H, Ar), 4.41 (d, $^3J_{HH}$ = 5.9 Hz, 2H, CH_2); ^{13}C NMR (101 MHz, DMSO) δ = 156.5 (q, $^2J_{CF}$ = 36 Hz, C═O), 140.2, 130.7, 130.2, 130.2, 126.4, 121.7 (Ar), 115.9 (q, $^1J_{CF}$ = 288 Hz, CF_3), 42.0 (d, $^4J_{CF}$ = 5 Hz, CH_2); ^{19}F NMR (376 MHz, DMSO-d_6) δ = −74.3 (s, CF_3); HR ESI MS m/z = 281.9741 ([M + H$^+$, ^{81}Br], $C_9H_8BrF_3NO^+$ calcd 281.9736).

*5′-O-(4,4′-Dimethoxytrityl)-5-(1-(3-((2,2,2-trifluoroacetamido)-methyl)phenyl)-1,2,3-triazol-4-yl)-2′-deoxyuridine (**2**).* To a stirred solution of *N*-(3-bromobenzyl)-2,2,2-trifluoroacetamide (423 mg, 1.5 mmol) in a mixture of ethanol and water (7:3, v/v, 3.0 mL) were added NaN_3 (97 mg, 1.5 mmol), CuI (28 mg, 0.15 mmol), *N*,*N*′-dimethylethylenediamine (20 mg, 0.22 mmol), and sodium ascorbate (15 mg, 0.07 mmol). The mixture was stirred under microwave irradiation (100 W) at 100 °C for 60 min. *N*,*N*′-Dimethylethylenediamine (20 mg, 0.22 mmol), sodium ascorbate (15 mg, 0.07 mmol), CuI (28 mg, 0.15 mmol), and nucleoside **1** (332 mg, 0.60 mmol) were added, and the mixture was stirred under microwave irradiation at 100 °C for 30 min. The reaction mixture was extracted with ethyl acetate (2 × 15 mL), and the combined organic phase was dried (Na_2SO_4) and concentrated under reduced pressure. The residue was purified by silica gel column chromatography (0−5% MeOH in CH_2Cl_2) and then coevaporated with toluene (10 mL) to afford the product **2** as a white foam (348 mg, 72%): R_f 0.5 (5% MeOH/CH_2Cl_2, v/v); ^{1}H NMR (DMSO-d_6, 400 MHz) δ 11.84 (br, 1H, NH(U)), 10.10 (t, J = 5.9 Hz, 1H, NHCO), 8.83 (s, 1H, CH triazole), 8.42 (s, 1H, H6), 7.89 (s, 1H, Ar), 7.85 (d, J = 8.0 Hz, 1H, Ar), 7.58 (t, J = 8.0 Hz, 1H, Ar), 7.42−7.37 (m, 3H, DMTr, Ar), 7.29−7.21 (m, 6H, DMTr), 7.19−7.11 (m, 3H, DMTr), 6.84−6.81 (m, 4H, DMTr), 6.20 (t, J = 6.4 Hz, 1H, H1′), 5.38 (d, J = 4.6 Hz, 1H, 3′−OH), 4.53 (d, J = 5.9 Hz, 2H, CH_2NH), 4.22 (m, 1H, H3′), 3.97 (m, 1H, H4′), 3.66 (s, 6H, 2 × OCH_3), 3.25−3.22 (m, 2H, H5′), 2.30−2.26 (m, 2H, H2′); ^{13}C NMR (DMSO-d_6, 100 MHz) δ 161.1, 158.0, 156.4 (q, $^2J_{CF}$ = 36 Hz, $COCF_3$), 149.5, 144.8, 139.9, 139.5, 136.6 (C6), 136.3, 135.5, 135.4, 130.1, 129.7, 129.6, 127.7, 127.6, 126.5, 119.9 (CH triazole), 119.1, 119.0, 115.9 (q, $^1J_{CF}$ = 288 Hz, CF_3), 113.1, 104.6, 85.7 (C4′), 85.3 (C1′), 70.4 (C3′), 54.9 (OCH_3), 42.2 (CH_2), 39.9 (C2′); ^{19}F NMR (DMSO-d_6, 376 MHz). δ −74.29 (CF_3); HR ESI MS m/z 821.2516 ([M + Na]$^+$, $C_{41}H_{37}F_3N_6O_8Na^+$ calcd 821.2517).

*3′-O-(P-(2-Cyanoethoxy)-(N,N-diisopropylamino)phosphinyl)-5′-O-(4,4′-dimethoxytrityl)-5-(1-(3-((2,2,2-trifluoroacetamido)methyl)-phenyl)-1,2,3-triazol-4-yl)-2′-deoxyuridine (**3**).* Nucleoside **2** (180 mg, 0.25 mmol) was coevaporated with anhydrous 1,2-dichloroethane (2 × 5 mL) and dissolved in anhydrous CH_2Cl_2 (5.0 mL). *N*,*N*-diisopropylethylamine (220 μL, 1.25 mmol), and 2-cyanoethyl-*N*,*N*-diisopropylamino chlorophosphite (180 μL, 0.75 mmol) were added and the reaction mixture was stirred at room temperature for 2 h. The reaction was quenched by the addition of 99.9% EtOH (2−3 drops), and the mixture was concentrated under reduced pressure. The residue was purified by column chromatography (0−2% MeOH in CH_2Cl_2) to afford the product **3** (125 mg, 54%) as a white foam: R_f 0.4 (2% MeOH in CH_2Cl_2); ^{31}P NMR ($CDCl_3$, 162 MHz) δ 149.1, 148.7; HR ESI MS m/z 1021.3625 ([M + Na]$^+$, $C_{50}H_{54}F_3N_8O_9PNa^+$ calcd 1021.3596).

*5-Azido-5′-(4,4′-dimethoxytrityl)-2′-deoxyuridine (**5**).* Nucleoside **4** (270 mg, 1.0 mmol) was coevaporated with anhydrous pyridine (2 × 10 mL) and redissolved in the same solvent (10 mL). 4,4′-Dimethoxytrityl chloride (410 mg, 1.20 mmol) was added, and the reaction mixture was stirred at room temperature for 14 h. The reaction was quenched by the addition of EtOH (99.9%, 3−4 drops), and the mixture was concentrated under reduced pressure. The residue was coevaporated with toluene (2 × 10 mL), dissolved in CH_2Cl_2 (30 mL), and washed with a saturated aqueous solution of $NaHCO_3$ (2 × 20 mL). The combined aqueous phase was extracted with CH_2Cl_2 (2 × 20 mL), and the combined organic phase was dried (Na_2SO_4) and concentrated under reduced pressure. The residue was purified by column chromatography (0−5% MeOH in CH_2Cl_2) to give the product **5** (240 mg, 42%) as a yellow solid: R_f 0.4 (5% MeOH in CH_2Cl_2); ^{1}H NMR ($CDCl_3$, 400 MHz) δ 9.27 (br s, 1H, NH), 7.51 (s, 1H, H6), 7.42−7.40 (m, 2H, DMTr), 7.33−7.23 (m, 7H, DMTr), 6.86−6.83 (m, 4H, DMTr), 6.28 (t, 1H, J = 6.6 Hz, H1′), 4.55 (m, 1H, H3′), 4.05 (m, 1H, H4′), 3.79 (s, 6H, 2 × OCH_3), 3.41 (dd, J = 10.4, 3.2 Hz, 1H, H5′), 3.33 (dd, J = 10.4, 3.2 Hz, 1H, H5′), 2.47 (m, 1H, H2′), 2.25 (m, 1H, H2′); ^{13}C NMR ($CDCl_3$, 100 MHz) δ 159.5 (C4), 158.8 (DMTr), 149.0 (C2), 144.5, 135.6, 135.4, 130.22, 130.20, 128.1 (DMTr), 127.4, 127.2 (C6, DMTr), 115.6 (C5), 113.4, (DMTr), 87.3 (DMTr), 86.4 (C4′) 85.5 (C1′), 72.2 (C3′), 63.4 (C5′), 55.4 (OCH_3), 41.3 (C2′); HR ESI MS m/z 594.1948 ([M + Na]$^+$, $C_{30}H_{29}N_5O_7Na^+$ calcd 594.1959).

*5′-(4,4′-Dimethoxytrityl)-5-(4-phenyl)-1,2,3-triazol-1-yl)-2′-deoxyuridine (**6**).* To a stirred solution of nucleoside **5** (170 mg, 0.29 mmol) and phenylacetylene (100 μL, 0.91 mmol) in a mixture of H_2O, *t*-BuOH, and pyridine (5 mL, 2:2:1, v/v/v) was added sodium ascorbate (60 mg, 0.30 mmol) and $CuSO_4{\cdot}5H_2O$ (25 mg, 0.10 mmol), and the reaction mixture was stirred at room temperature for 3 h. Ethyl acetate (30 mL) was added, and the mixture was washed with H_2O (20 mL) and a saturated aqueous solution of $NaHCO_3$ (20 mL). The combined aqueous phase was extracted with ethyl acetate (2 × 15 mL), and the combined organic phase was dried (Na_2SO_4) and concentrated under reduced pressure. The residue was purified by column chromatography (0−5% MeOH in CH_2Cl_2) to afford the nucleoside **6** (130 mg, 65%) as a pale yellow solid: ^{1}H NMR (DMSO-d_6, 400 MHz) δ 12.15 (s, 1H, NH), 8.53 (s, 1H, CH triazole), 8.27 (s, 1H, H6), 7.83 (d, J = 7.6 Hz, 2H, Ph), 7.46 (t, J = 7.6 Hz, 2H, Ph), 7.38−7.34 (m, 1H, Ph), 7.29−7.27 (m, 2H, DMTr), 7.23−7.19 (m, 2H, DMTr), 7.19−7.12 (m, 5H, DMTr), 6.82−6.79 (m, 4H, DMTr), 6.18 (t, J = 6.4 Hz, 1H, H1′), 5.37 (d, J = 4.4 Hz, 1H, 3′−OH), 4.27 (m, 1H, H3′), 3.95 (m, 1H, H4′), 3.67 (s, 6H, OCH_3), 3.25 (dd, J = 10.4, 5.2 Hz, 1H, H5′), 3.11 (dd, J = 10.4, 2.6 Hz, 2H, H5′), 2.39−2.30 (m, 2H, H2′); ^{13}C NMR (DMSO-d_6, 100 MHz) δ 158.6 (C4), 157.9, (DMTr), 149.1 (C2), 146.2 (C triazole), 144.5 (DMTr), 136.9 (C6), 135.3, 135.1, 130.1, 129.5, 129.4, 128.8, 127.9, 127.7, 127.4, 126.5, (Ph, DMTr), 125.2 (Ph), 123.0 (CH triazole), 113.0 (DMTr, C5), 85.9, 85.7, 85.5 (C1′, C4′, DMTr), 70.2 (C3′), 63.5 (C5′), 54.8 (OCH_3), 40.0 (C2′); HR ESI MS m/z 696.2398 ([M + Na]$^+$, $C_{38}H_{35}N_5O_7Na^+$ calcd 696.2429).

*3′-O-(P-(2-Cyanoethoxy)-N,N′-diisopropylaminophosphinyl)-5′-O-(4,4′-dimethoxytrityl)-5-(4-phenyl)-1,2,3-triazol-1-yl)-2′-deoxyuridine (**7**).* The nucleoside **6** (120 mg, 0.17 mmol) was coevaporated with anhydrous 1,2-dichloroethane (2 × 5 mL) and dissolved in anhydrous CH_2Cl_2 (5 mL). *N*,*N*-Diisopropylammonium tetrazolide (72 mg, 0.36 mmol) and 2-cyanoethyl *N*,*N*,*N*′,*N*′-tetraisopropylphosphoramidite (120 μL, 0.35 mmol) were added, and the mixture was stirred at room temperature for 14 h. The reaction was quenched by the addition of 99.9% EtOH (4 drops), and the mixture was concentrated under reduced pressure. The residue was purified by column chromatography (0−2% MeOH in CH_2Cl_2) to afford the product **7** (105 mg) as a white foam containing some hydrolyzed phosphitylation reagent. The compound was used without further purification in the ON synthesis: R_f 0.5 (3% MeOH in CH_2Cl_2); ^{31}P NMR ($CDCl_3$, 162 MHz) δ 149.1, 148.8; HR ESI MS m/z 874.3685 ([M + H]$^+$, $C_{47}H_{53}N_7O_8PH^+$ calcd 874.3688).

*5′-(4,4′-Dimethoxytrityloxymethyl)-5-phenyl-2′-deoxyuridine (**10**).* To a stirred solution of 5-phenyl-2′-deoxyuridine **9** (268 mg, 0.88 mmol) in a mixture of anhydrous CH_3CN and pyridine (17 mL, 1:1, v/v) was added 4,4′-dimethoxytrityl chloride (462 mg, 1.36 mmol). The mixture was stirred at room temperature for 4 h and then quenched by the addition of MeOH (4 mL). The mixture was concentrated under reduced pressure, and the residue was dissolved in CH_2Cl_2 (100 mL). The organic phase was washed with water (20 mL) and a saturated aqueous solution of $NaHCO_3$ (20 mL). The organic phase was dried ($MgSO_4$) and concentrated under reduced pressure. The residue was purified by flash chromatography (10−100% ethyl acetate in cyclohexane) to afford the product **10** (254 mg, 47%) as a white amorphous solid: R_f 0.30 (5% MeOH in CH_2Cl_2); ^{1}H NMR (400 MHz, DMSO-d_6) δ 11.60 (s, 1H, NH), 7.66 (s, 1H, H6), 7.30−7.15 (m, 14H, Ph, DMTr), 6.77 (m, 4H, DMTr), 6.23 (t, J = 6.8 Hz, 1H, H1′), 5.34 (d, J = 4.4 Hz, 1H, 3′−OH), 4.29 (m, 1H, H3′), 3.93

dx.doi.org/10.1021/jo4025896 | J. Org. Chem. 2014, 79, 2854−2863

(m, 1H, H4′), 3.69 (s, 6H, 2 × OCH_3), 3,19 (dd, J = 10.0 Hz, 4.8 Hz, 1H, H5′), 3.13 (dd, J = 10.0 Hz, 4.8 Hz, 1H, H5′), 2.34 (m, 1H, H2′), 2.23 (m, 1H, H2′); ^{13}C NMR (101 MHz, DMSO-d_6) δ 162.0 (C4), 158.0 (DMTr), 149.9 (C2), 144.6 (DMTr), 137.1 (C6), 135.2, 132.7, 129.6, 129.5, 128.2, 127.9, 127.8, 127.5, 127.2, 126.6 (DMTr, Ph), 114.1 (C5), 113.1 (DMTr), 85.7 (C4′), 84.7 (C1′), 70,6 (C3′), 63.8 (C5′), 55.0 (OCH_3), 40.0 (C2′). HR ESI MS m/z 629.2248 ([M + Na]$^+$, $C_{36}H_{34}N_2O_7Na^+$ calcd 629.2264).

3′-O-(P-(2-Cyanoethoxy)-N,N′-diisopropylaminophosphinyl)-5′-(4,4′-dimethoxytrityl)-5-phenyl-2′-deoxyuridine (11). Nucleoside **10** (136 mg, 0.224 mmol) was coevaporated with anhydrous 1,2-dichloroethane (2 × 5 mL) and dissolved in anhydrous CH_2Cl_2. *N,N*-Diisopropylammonium tetrazolide (89 mg, 0.448 mmol) and 2-cyanoethyl-*N,N,N′,N′*-tetraisopropylphosphoramidite (142 μL, 0.448 mmol) were added, and the mixture was stirred at room temperature for 2 h. The reaction was quenched by the addition of 99.9% EtOH (1 mL), and the mixture was concentrated under reduced pressure. The residue was purified by column chromatography (0−5% MeOH in CH_2Cl_2) to give the product **11** (110 mg) as a white foam containing some hydrolyzed phosphitylation reagent. The compound was used without further purification in the ON synthesis: R_f 0.70 (10% CH_3OH in CH_2Cl_2); ^{31}P NMR ($CDCl_3$, 162 MHz) δ 149.01, 148.52; HR ESI MS m/z 829.3334 ([M + Na]$^+$, $C_{45}H_{51}N_4O_8PNa^+$ calcd 829.3337).

Oligonucleotide Synthesis. Oligonucleotide synthesis was carried out on an automated DNA synthesizer following the phosphoramidite approach. Synthesis of oligonucleotides was performed on a 0.2 μmol scale using the amidites **3**, **7**, and **11** as well as the corresponding commercial 2-cyanoethyl phosphoramidites of the natural 2′-deoxynucleosides and the amidite for **W**.[8] The synthesis followed the regular protocol for the DNA synthesizer. For the modified phosphoramidites, a prolonged coupling time of 15 min was used. 1*H*-Tetrazole was used as the activator, and coupling yields for all 2-cyanoethyl phosphoramidites were >90%. The 5′-*O*-DMT-ON oligonucleotides were removed from the solid support by treatment with concentrated aqueous ammonia at 55 °C for 16 h, which also removed the protecting groups. The oligonucleotides were purified by reversed-phase HPLC on a Waters 600 system using a XBridge OST C18 column, 19 × 100 mm, 5 μm + precolumn: XBridge 10 × 10 mm, 5 μm. Temperature 50 °C; Buffer A: 0.05 M triethylammonium acetate pH 7.4. Buffer B: MeCN/H_2O (3:1). Program used: 2 min 100% A, 100%−30%:0%−70% A:B over 17 min, 4 min 100% B, 6 min 100% A. Flow 5 mL/min. All fractions containing 5′-*O*-DMTr protected oligonucleotide were collected and concentrated. The products were detritylated by treatment with 80% aqueous acetic acid (100 μL) for 30 min at room temperature and subsequently diluted with water (100 μL). Aqueous solutions of sodium acetate (3 M, 15 μL) and sodium perchlorate (5 M, 15 μL) were added followed by acetone (1 mL). Oligonucleotides were allowed to precipitate overnight at −20 °C. After centrifugation at 12000 rpm, 10 min at 4 °C, the supernatant was removed, and the pellet was washed with cold acetone (2 × 1 mL), dried by heating (55 °C) under a flow of nitrogen, and dissolved in pure water (1000 μL). Constitution of the synthesized ONs was verified by ion-exchange chromatography and MALDI-MS. The concentration was determined by UV at 260 nm. The extinction coefficients of the modified ONs were estimated from a standard method using micromolar extinction coefficients for the monomers. For **Y** this was determined on a small amount of detritylated **6**; ε_{260} = 14.0. For **X** and **Z** were used the coefficients of **W**[8] and of dT, respectively.

Thermal Denaturation Experiments. UV melting experiments were carried out on a UV spectrometer. Samples were dissolved in a medium salt buffer containing 2.5 mM Na_2HPO_4, 5 mM NaH_2PO_4, 100 mM NaCl, and 0.1 mM EDTA at pH = 7.0 with 1.5 μM concentrations of the two complementary sequences. The increase in absorbance at 260 nm as a function of time was recorded while the temperature was increased linearly from 10 to 75 °C at a rate of 1.0 °C/min by means of a Peltier temperature programmer. The melting temperature was determined as the local maximum of the first derivatives of the absorbance vs temperature curve. The melting curves were found to be reversible. All determinations are averages of at least duplicates within ±0.5 °C.

CD Spectroscopy. CD spectra (200−350 nm) were recorded on a JASCO J-815 CD-spectrometer as an average of 5 scans using a split of 2.0 nm, and a scan speed of 50 nm/min. Samples were dissolved in a medium salt buffer containing 2.5 mM Na_2HPO_4, 5 mM NaH_2PO_4, 100 mM NaCl, and 0.1 mM EDTA at pH = 7.0 with 3.0 μM concentrations of the two complementary oligonucleotide sequences, heated to 80 °C, and cooled to 10 °C. Quartz optical cells with a path length of 5.0 mm were used.

Ab Initio Calculations. The energy profiles were calculated by relaxed coordinate scans of the dihedral angles between the uracil ring and the planar 5-substituents. The computations were performed at the LMP2 level with the 6-31G(d,p) basis set using the Jaguar V7.8 software package within the Maestro Molecular Modeling interface V9.2.109. The torsional sampling was performed by a 2° increment of the dihedral angle (from 0° to 360°) to obtain 181 minimized structures, the relative potential energies of which were plotted against the corresponding dihedral angle.

Global Minimum Structures. The global minimum structures were found from 5 ns molecular dynamics simulations using the all-atom AMBER* force field and the Polak-Ribiere Conjugate Gradient (PRCG) method. The duplexes were built in B-type geometries, and initial Monte Carlo torsional samplings (MCMM) were performed to generate 1000 structures, which were minimized into local minima. The lowest energy structures for each of the duplexes were used for subsequent MD simulations. The MD simulations were performed at 300 K. SHAKE all bonds to hydrogen was imposed in order to increase the time step to 2.2 fs, and an equilibration time of 100 ps was used to stabilize the calculations. A multiple minimization of the 500 sampled structures was performed to obtain a converged global minimum structure.

■ ASSOCIATED CONTENT

Ⓢ Supporting Information

MALDI-TOF data for oligonucleotides. Additional MD-simulations. Selected NMR spectra. This material is available free of charge via the Internet at http://pubs.acs.org.

■ AUTHOR INFORMATION

Corresponding Author

*Fax: +45 66158780. E-mail: pouln@sdu.dk.

Notes

The authors declare no competing financial interest.

■ ACKNOWLEDGMENTS

The project was supported by The Danish National Research Foundation, The Danish Council for Independent Research/Natural Sciences (FNU) and Technology and Production Sciences (FTP), and Villum Kann Rasmussen Fonden.

■ REFERENCES

(1) Zamecnik, P. C.; Stephenson, M. L. *Proc. Natl. Acad. Sci. U.S.A.* **1978**, *75*, 280−284.

(2) Crooke, S. T.; Wickers, T.; Lima, W.; Wu, H. In *Antisense Drug Technology: Principle, Strategies and Applications*, 2nd ed.; Crooke, S. T., Ed.; CRC: Boca Raton, 2008; pp 3−46.

(3) Kurreck, J. *Eur. J. Biochem.* **2003**, *270*, 1628−1644.

(4) Deleavey, G. F.; Damha, M. J. *Chem. Biol.* **2012**, 937−954.

(5) Lin, K. −Y.; Jones, R. J.; Matteucci, M. J. *J. Am. Chem. Soc.* **1995**, *117*, 3873−3874.

(6) Froehler, B. C.; Wadwani, S.; Terhorst, T. J.; Gerrard, S. R. *Tetrahedron Lett.* **1992**, *33*, 5307−5310.

(7) Freier, S. M.; Altmann, K.-H. *Nucleic Acids Res.* **1997**, *25*, 4429−4443.

(8) Kocalka, P.; Andersen, N. K.; Jensen, F.; Nielsen, P. *ChemBioChem* **2007**, *8*, 2106−2116.

(9) Tornøe, C. W.; Christensen, C.; Meldal, M. *J. Org. Chem.* **2002**, *67*, 3057−3064.
(10) Rostovtsev, V. V.; Green, L. G.; Fokin, V. V.; Sharpless, K. B. *Angew. Chem., Int. Ed.* **2002**, *41*, 2596−2599.
(11) Gramlich, P. M. E.; Wirges, C. T.; Manetto, A.; Carell, T. *Angew.Chem., Int. Ed.* **2008**, *47*, 8350−8358.
(12) Amblard, F.; Cho, J. H.; Schinazi, R. F. *Chem. Rev.* **2009**, *109*, 4207−4220.
(13) El-Sagheer, A. H.; Brown, T. *Chem. Soc. Rev.* **2010**, *39*, 1388−1405.
(14) Østergaard, M. E.; Guenther, D. C.; Kumar, P.; Baral, B.; Deobald, L.; Paszczynski, A. J.; Sharma, P. K.; Hrdlicka, P. J. *Chem. Commun.* **2010**, *46*, 4929−4931.
(15) Shaikh, K. I.; Madsen, C. S.; Nielsen, L. J.; Jørgensen, A. S.; Nielsen, H.; Petersen, M.; Nielsen, P. *Chem.—Eur. J.* **2010**, *16*, 12904−12919.
(16) Jørgensen, A. S.; Shaikh, K. I.; Enderlin, G.; Ivarsen, E.; Kumar, S.; Nielsen, P. *Org. Biomol. Chem.* **2011**, *9*, 1381−1388.
(17) Kumar, P.; Shaikh, K. I.; Jørgensen, A. S.; Kumar, S.; Nielsen, P. *J. Org. Chem.* **2012**, *77*, 9562−9573.
(18) Andersen, N. K.; Chandak, N.; Brulikova, L.; Kumar, P.; Jensen, M. D.; Jensen, F.; Sharma, P. K.; Nielsen, P. *Bioorg. Med. Chem.* **2010**, *18*, 4702−4710.
(19) Andersen, N. K.; Døssing, H.; Jensen, F.; Vester, B.; Nielsen, P. *J. Org. Chem.* **2011**, *76*, 6177−6187.
(20) Kumar, P.; Chandak, N.; Nielsen, P.; Sharma, P. K. *Bioorg. Med. Chem.* **2012**, *20*, 3843−3849.
(21) Heystek, L. E.; Zhou, H.-Q.; Dande, P.; Gold, B. *J. Am. Chem. Soc.* **1998**, *120*, 12165−12166.
(22) Østergaard, M. E.; Kumar, P.; Baral, B.; Raible, D. J.; Kumar, T. S.; Anderson, B. A.; Guenther, D. C.; Deobald, L.; Paszczynski, A. J.; Sharma, P. K.; Hrdlicka, P. J. *ChemBioChem* **2009**, *10*, 2740−2743.
(23) Hurley, D. J.; Tor, Y. *J. Am. Chem. Soc.* **1998**, *120*, 2194−2195.
(24) Gourdain, S.; Petermann, C.; Harakat, D.; Clivio, P. *Nucleosides, Nucleotides Nucleic Acids* **2010**, *29*, 542−546.
(25) (a) Bigge, C. F.; Mertes, M. P. *J. Org. Chem.* **1981**, *46*, 1994−1997. (b) Western, E. C.; Daft, J. R.; Johnson, E. M.; Gannett, P. M.; Shaughnessy, K. H. *J. Org. Chem.* **2003**, *68*, 6767−6774. (c) Fresneau, N.; Hiebel, M.-A.; Agrofoglio, L. A.; Berteina-Raboin, S. *Molecules* **2012**, *17*, 14409−14417.
(26) (a) Sartori, G.; Enderlin, G.; Hervé, G.; Len, C. *Synthesis* **2012**, *44*, 767−772. (b) Sartori, G.; Hervé, G.; Enderlin, G.; Len, C. *Synthesis* **2013**, *45*, 330−333. (c) Gallagher-Duval, S.; Hervé, G.; Sartori, G.; Enderlin, G.; Len, C. *New J. Chem.* **2013**, *37*, 1989−1995.
(27) (a) Burley, G. A.; Gierlich, J.; Mofid, M. R.; Nir, H.; Tal, S.; Eichen, Y.; Carell, T. *J. Am. Chem. Soc.* **2006**, *128*, 1398−1399. (b) Gierlich, J.; Burley, G. A.; Gramlich, P. M. E.; Hammond, D. M.; Carell, T. *Org. Lett.* **2006**, *8*, 3639−3642.
(28) Beyer, C.; Wagenknecht, H.-A. *Chem. Commun.* **2010**, *46*, 2230−2231.
(29) (a) Wagner, C.; Wagenknecht, H.-A. *Chem.—Eur. J.* **2005**, *11*, 1871−1876. (b) Jacobsen, M. F.; Ferapontova, E. E.; Gothelf, K. V. *Org. Biomol. Chem.* **2009**, *7*, 905−908. (c) Fukuda, M.; Nakamura, M.; Takada, T.; Yamana, K. *Tetrahedron Lett.* **2010**, *51*, 1732−1735. (d) Park, S. M.; Nam, S.-J.; Jeong, H. S.; Kim, W. J.; Kim, B. H. *Chem.—Asian J.* **2011**, *6*, 487−492.